Materials Physics and Mechanics. 2023;51(2): 50-57
Research article
http://dx.doi.org/10.18149/MPM.5122023_5

Submitted: November 28, 2022
Approved: December 2, 2022
Accepted: March 3, 2023

Spectra of crystal curvature in terms of EBSD data to assess martensite fraction in bainitic steel

A.A. Zisman [1,2] ✉, S.N. Petrov [1,2], N.Y. Zolotorevsky [1], N.Y. Ermakova [1]

[1] Peter the Great St.Petersburg Polytechnic University, St. Petersburg, Russia

[2] CRISM "Prometey"-National Research Center "Kurchatov Institute", St. Petersburg, Russia

✉ crism_ru@yahoo.co.uk

Abstract. A martensitic or bainitic structure of low-carbon steel provides its high strength and fracture toughness combined with good weldability. At the same time, the phase composition of such materials depends on the cooling rate in quenching and hence becomes rather non-uniform in case of thick semi-products. Accordingly, to answer a challenging question of how this issue affects the metal properties, relevant methods of local structural analysis are required. To assess martensite fractions in low carbon bainitic steel quenched at different cooling rates, statistics of the crystal curvature in terms of EBSD data is analyzed. Results are verified by independent data on the transformation kinetics recorded by dilatometry and characteristic coupling of the transformation variants admitted by the interphase orientation relationship.
Keywords: martensite, bainite, crystal curvature, EBSD, transformation kinetics

Acknowledgement. *The authors acknowledge a financial support of this work by the Russian Science Foundation, project No 22-19-00627. Microtructural studies were carried out on the equipment of the Core shared research facilities "Composition, structure and properties of structural and functional materials" of the NRC "Kurchatov Institute" - CRISM "Prometey".*

Citation: Zisman AA, Petrov SN, Zolotorevsky NY, Ermakova NY. Spectra of crystal curvature in terms of EBSD data to assess martensite fraction in bainitic steel. *Materials Physics and Mechanics*. 2023;51(2): 50-57. DOI: 10.18149/MPM.5122023_5.

Introduction

A martensitic or bainitic structure of low-carbon steel provides its high strength and fracture toughness, combined with good weldability. At the same time, the phase composition of such materials depends on the cooling rate in quenching and hence becomes rather non-uniform in case of *thick* semi-products. Accordingly, to answer a challenging question of how this issue affects the metal properties, relevant methods of local structural analysis are required. If some constituent is minor (e.g., martensite islands in a mostly bainitic structure), its accurate evaluation by the usual optical microscopy of etched sections will be hardly possible. A popular alternative is EBSD [1] that maps crystal orientations at periodically arranged separate points and, subsequently, related curvature (orientation gradient) that is sensitive to the local dislocation density. Since the latter notably differ in dissimilar phases (e.g., bainite and martensite), simple scalar measures for the curvature [2-5] have been applied to resolve the problem.

The most used curvature characteristics are KAM (kernel average misorientation) and GAM (grain average misorientation). The former one averages magnitudes of misorientation angles between each data point and a predefined number of its neighbors. To enhance spatial

resolution of KAM, only the first coordination layer will be further considered. However, such a measure depends not only on the bulk lattice curvature but also on orientation jumps at *interfaces.* To avoid related errors, a proper tolerance angle θ_t should be selected that will exclude neighboring points with $\theta > \theta_t$. Moreover, θ_t enables partitioning of the orientation map into finite domains separated by closed boundaries. Thus, unlike an essentially local and rather noisy KAM, GAM is introduced to express its average value over any domain and hence to specify the latter *as a whole*. To properly treat such structural elements, the EBSD scanning step Δ should be relevant to the considered structure. For example, if lath widths in martensite vary around 300 nm, Δ<100 nm at most is desired. It is worth noting as well that both KAM and GAM are expressed in angular units (e.g., degrees) unlike the physical dimension of curvature [angle/length]. However, if spacing Δ is fixed, these characteristics are proportional to the orientation gradient and hence suitable for curvature imaging.

The mapping of GAM or another related parameter still has serious limitations. First, it is not a trivial question of how to predefine certain curvature ranges indicative of various constituents. Second, even if such ranges are somehow selected, discrimination between domains of different structural types is not always accurate because their curvature variations may overlap. In the present paper, to mitigate the above-mentioned drawbacks, we will extract from the treated area an *overall* spectrum of curvature rather than its *local* values for specific elements. The obtained experimental results and those earlier reported in [6] indicate that shapes of such spectra are sufficiently sensitive to minor phase constituents, even if their distinction in curvature is modest. Furthermore, respective estimates can be verified by their comparison to the transformation kinetics as provided by dilatometry.

One more way to make use of EDSD data in analysis of martensite or bainite structure is to assess specific interfacial areas between admitted variants of the orientation relationship (OR). According to [7-9], statistics of the variant coupling depends on fractions of martensite and bainite as well as on specific types of the latter. However, to accurately distinguish individual variants, an actual rather than virtual reference OR should be applied. Following [10], we will extract OR from a set of interfacial disorientation because this method excludes errors due to the substructure of parent austenite grains and strongly accelerates computations. Besides, the same OR will be used to select in the transformed structure the above-mentioned tolerance angle θ_t that should correspond to the least inter-variant misorientation.

Material and experimental methods

Chemical composition of the considered steel (wt.%: 0.090C, 2.65(Ni + Cu), 0.83(Cr + Mo), 0.27Si, 0.56Mn, 0.02V) suggests in its quenched state a mostly bainitic structure for a rather wide range of cooling rates (2 to 50 °C/s) covering various industrial conditions. Reheated to 950 °C and then hold for 100 s, steel specimens (Ø5×10 mm) have been quenched at cooling rates of 3 and 70 °C/s on Dil 805-A/D dilatometer. The transformation kinetics for these specimens is then represented in terms of their thermal expansions.

Planar sections were prepared by conventional metallographic procedures and additionally subjected to electrolytic polishing; then the transformed structures have been analyzed by EBSD with a scanning step of 50 nm on SEM Lyra 3-XM at an accelerating voltage of 20 kV. Lattice orientations at discrete data points arranged according to a virtual square grid have been determined with an angular accuracy of about one degree within areas of 100μm in width and height by means of own AZTEC software of the SEM.

In addition to the orientation data further treated according to the next section, the band contrast (BC) of EBSD sensitive to lattice defects has been imaged. In a sense, its maps substitute microstructure images provided by the conventional chemical etching.

Treatment of experimental data

To enhance accuracy of determined martensite fractions in the quenched bainitic steel, raw data of dilatometry and EBSD have been reprocessed as follows.

Dilatometry. Unlike the simplified lever rule based on local *tangent lines* to the dilatometric curve, the transformation degree has been quantified according to [11] with allowance for temperature dependences of the thermal expansion coefficient in both the parent and product phases. When neglecting this issue, the transformation start temperature would be overestimated by 20 to 40 °C. Besides, derivatives of the recorded transformation degree with respect to temperature have been plotted to clearly reveal its bimodal (two-phase) character, if any. Since at the lower cooling rate (3 °C/s) the transformation kinetics displays no distinct sign of the banite-to-martensite transition, a small fraction of the latter phase is roughly attributed to temperatures below certain M_s estimated according to [12] in terms of the chemical composition. Although at the higher cooling rate (70 °C/s) such a transition near M_s virtually indicating the martensite start becomes apparent and suggests comparable fractions of considered phases, the refined final estimates will be based on EBSD data.

EBSD. To get tolerance angle θ_t needed in mapping GAM of individual bainite and martensite crystals, actual OR at the applied cooling rates have been specifically derived according to [10] from interfacial misorientations. Based on the same OR, mutual lattice rotations of its coupled variants V_1/V_i (I = 2, 3, …, 24) have been determined with angular accuracy of one degree to evaluate the corresponding fractions of inter-variant boundaries in terms of their lengths on the section plane. To assess volume fractions of constituent phases as considered in the introduction section, the spectra of GAM further denoted by G are extracted from experimental bar charts for its probability density p over intervals of 0.02° width. Parts of p due to bainite and martensite are determined as follows.

The main bainite contribution to p is approximated by a continuous function, whereas the residual due to other constituents is found by subtraction of this approximation from p. The considered function is sought in a form

$$B = \alpha f, \qquad 0 < \alpha \leq 1, \tag{1}$$

where

$$f = (2\pi)^{-1/2}(G\sigma)^{-1} exp\,\{-(Ln(G) - \mu)^2/(2\sigma^2)\} \tag{2}$$

is a lognormal function of G. It was necessary to rescale f since its integral over the whole range of G reaches unity that generally exceeds an integral of *constituent B*. The lognormal function is used since it is relevant to a natural effect of the current transformation degree on its further rate and has suitable properties (a positive definition range and a longer right tail). In a sense, such an effect resembles the popular example of a repeatedly crushed solid, where the number and dimensions of debris at any step are predefined by those at previous steps. Parameters μ, σ and α are sought to get

$$\sum_{i=m}^{n}(B_i - p_i)^2 = min \tag{3}$$

over an appropriate region of axis G (sequence of G intervals $m \leq i \leq n$). At the low cooling rate, a very small amount of martensite, if any, should not affect the mode (maximum position) of experimental p. Therefore, this mode is ascribed to B for predominant bainite. Function B is then fitted to the plot of p except for its lowest values at the *right* tail, corresponding to the maximum level of curvature. The same region is then used to assess the martensite fraction. In case of the rapid quenching that admits a notable fraction of martensite, B is fitted to a part of the *left* tail before a distinct inflection point due to influence of the harder constituent. In both cases, a nonlinear least-square method is employed to find three parameters of function B.

Results and discussion

Figure 1 represents temperature dependences of the transformed fractions and their derivatives at the two cooling rates. Owing to a smooth transformation curve confirmed by a mono-modal shape of the derivative, no sign of martensite is perceptible at the slow quenching. Thus, a pure bainite should predominate, whereas temperature of about 670 °C at its nucleation suggests a granular type of this phase.

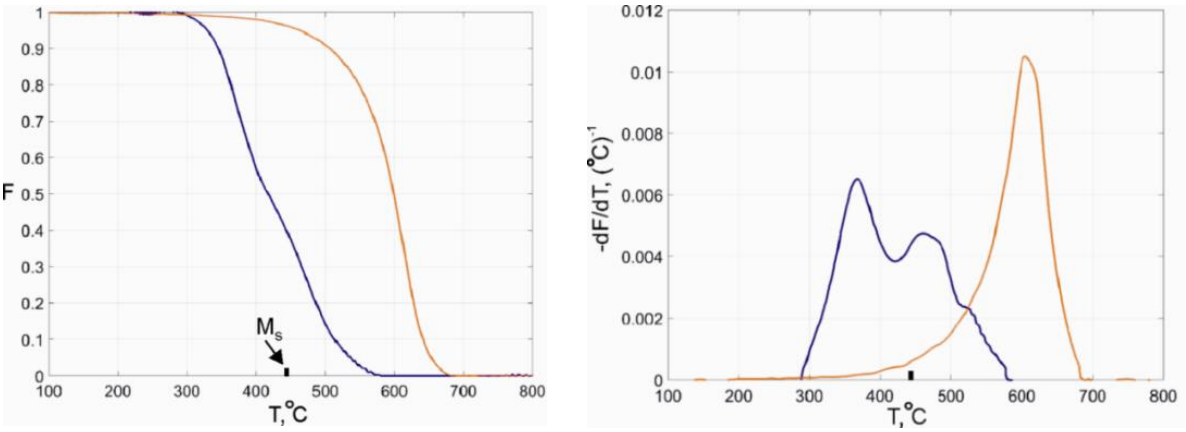

(a) (b)

Fig. 1. Temperature dependences of the transformation degree (a) and its derivative (b) at cooing rates of 3 and 70 °C/s. The rates correspond to red and blue lines, respectively

Formally, few per cent of martensite and residual austenite can comply with a temperature range below theoretical M_s owing to the carbon repulsion into austenite during the bainitic transformation [13-15]. However, this reservation must be verified by an independent method. In case of the rapid quenching, the martensite appearance near M_s becomes apparent due to both an inflection region in Fig. 1a and a bi-modal distribution in Fig. 1(b). In this case, the nucleation of bainite below 600 °C admits its low-temperature (lath) sort. At the same time, to confirm the latter and accurately quantify fractions of the coexisting phases, EBSD data should be analyzed.

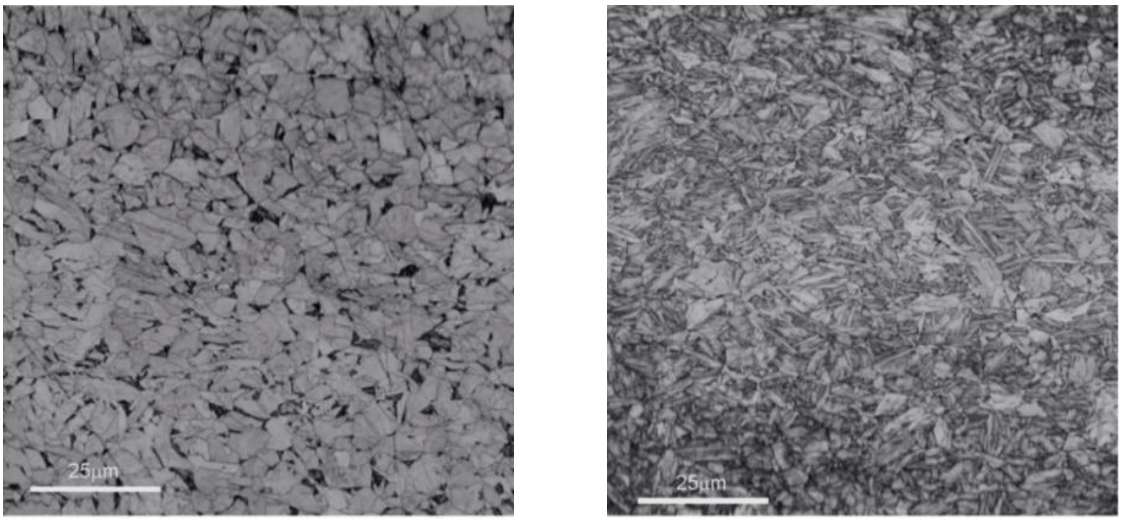

(a) (b)

Fig. 2. EBSD band contrast maps of steel quenched from 950°C at cooling rates of (a) 3 and (b) 70°C/s

BC maps of EBSD shown in Fig. 2 qualitatively support the previous assumptions. Indeed, at the low cooling rate the most part of the transformed structure corresponds to the granular bainite although small fractions of dispersed dark domains and light grains may be attributed to a martensite/austenite constituent and ferrite, respectively. At the high cooling rate the BC map looks as an expected mixture of bainite and martensite where the former phase mostly gets lath morphology since the temperature of its nucleation has been notably reduced with respect to the previous case.

According to GAM maps represented in Fig. 3, the average level of crystal curvature increases at the rapid quenching, as expected. At the same time, the contrast of these images is not sufficient to accurately quantify fractions of the coexisting bainite and martensite. That is why, to refine analysis, the curvature statistics becomes indispensable.

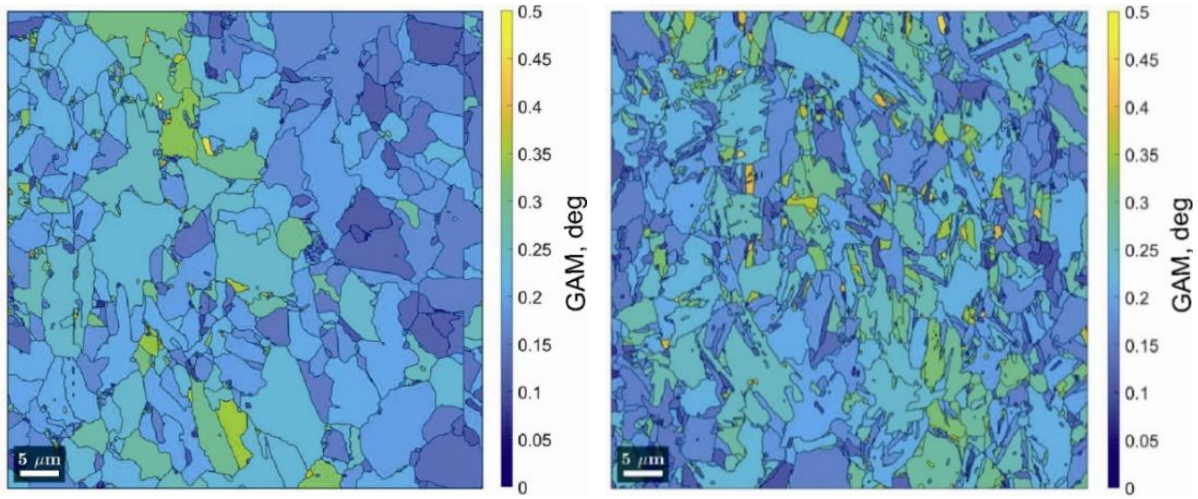

(a) (b)

Fig. 3. GAM maps of steel quenched from 950°C at cooling rates of (a) 3 and (b) 70 °C/s

Figure 4 represents GAM spectra for the considered cooling rates. As expected, the spectrum at faster cooling spreads to right, that is, to stronger curvature. Dashed lines in these plots correspond to bainite constituents fitted according to Section 3 to experimental p. Note that despite the slow quenching, the lower part of the right tail in Fig. 4(a) distinctly deviates from the bainitic curve and hence suggests some martensitic residual. As to some deviation of p from B at the lowest level of curvature ($G < 0.2$ deg), this may be partly due to an insignificant fraction of ferrite and will not affect treatment of a short martensite range at the *right* tail. The fitted lognormal approximations display relevant properties. Indeed, in both cases the corresponding bainite constituents are situated within the same range of G; moreover, the positions of their maximums prove to be rather close to each other. According to the difference between lath (low temperature) and granular types of bainite in dislocation density, a slightly higher mode of B at the rapid cooling (Fig. 4(b)) also could be expected.

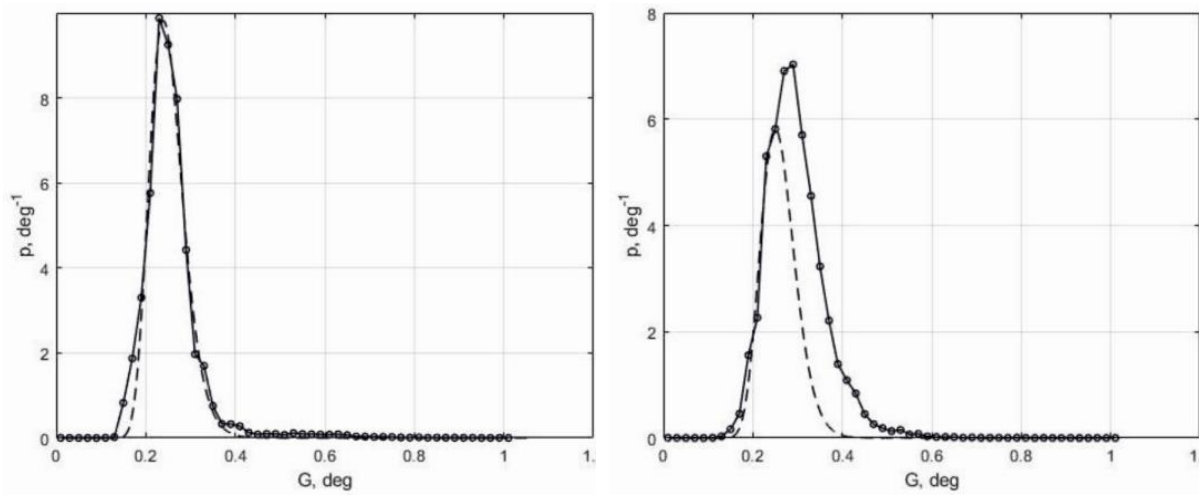

Fig. 4. GAM spectra of steel quenched from 950 °C at cooling rates (a) 3 and (b) 70 °C/s. Rescaled lognormal functions (dashed lines) fitted to experimental data approximate respective bainite constituents

Bainite and martensite fractions evaluated by the dilatometric technique and derived from EBSD data at different cooling rates are listed in Table 1. Although results based on virtual temperature M_s due to the chemical composition of steel [12] could not pretend to high accuracy, correspondence between estimates by the two methods proves to be better than could be expected. As to a lesser martensite fraction at the high cooling rate according to the former approach based on calculated M_s, the latter is hardly relevant here because it presumes the martensite appearance *first* rather than its nucleation at the preformed bainite. It is worth noting as well that evaluation of bainite fraction ignores an insignificant contribution of ferrite possible in the considered steel at the cooling rate of 3 °C/s.

Table 1. Bainite and martensite fractions (%) evaluated by two methods

Method	Cooling rate, °C/s	Bainite	Martensite
Dilatometry*	3	96.4	3.6
	70	43.2	56.8
EBSD	3	95.5	4.5
	70	55.5	44.5

* Rough estimates based on a virtual temperature of martensite start

Statistics of OR variant coupling represented in Fig. 5 also qualitatively comply with the previous analysis. Thus, according to [7,8], predominance of V_1/V_8 couple and modest frequency of V_1/V_2 are characteristic for bainite nucleated at higher temperatures peculiar the slower cooling. At the rapid cooling and hence lesser temperature of the transformation start, as noted in the same reference, the strongly increased V_1/V_2 and reduced V_1/V_8 couple frequencies indicate another (low temperature) sort of bainite. At the same time, these findings are hardly relevant to the considered martensite because the latter appears after a significant fraction of the preformed bainite. Besides, according to [16], in some steels the couple V_1/V_4 rather than V_1/V_8 can dominate in high temperature bainites.

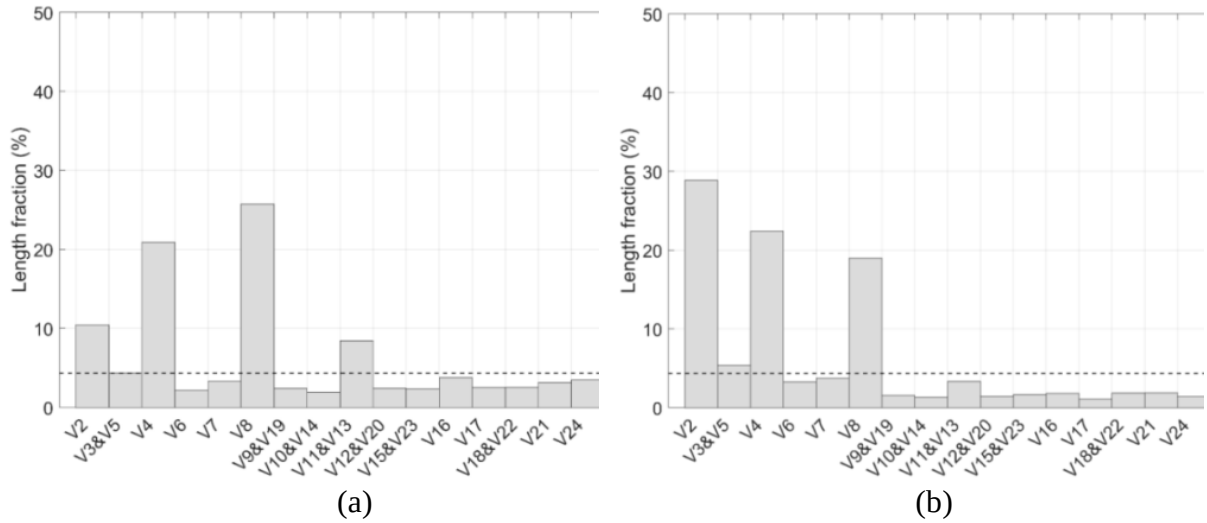

Fig. 5. Spectra of OR variant coupling in steel quenched from 950°C at cooling rates (a) 3 and (b) 70°C/s. Dotted lines correspond to the random variant coupling

Conclusion

The crystal curvature spectra derived from EBSD data reflect the difference between bainite and martensite in dislocation density, and hence enable assessment of martensite fractions in low carbon bainitic steel quenched at low and high cooling rates. This method applicable to industrial steel semi-products gains in significance when a minor structural constituent cannot be properly quantified by conventional metallographic techniques.

References

1. Adams BL, Wright SI, Kunze K. Orientation imaging: The emergence of a new microscopy. *Metallurgical and Materials Transactions*. 1993;A24: 819–831.
2. Breumier S, Martinez Ostormujof T, Frincu B, Gey N, Couturier A, Loukachenko N, Abaperea PE, Germain L. Leveraging EBSD data by deep learning for bainite, ferrite and martensite segmentation. *Materials Characterization*. 2022;186: 111805.
3. Santos DB, Camey K, Barbosa R, Andrade MS, Escobar DP. Complex phase quantification methodology using electron backscatter diffraction (EBSD) on low manganese high temperature processed (HTP) microalloyed steel. *Journal of Materials Research and Technology*. 2022;8(2): 2423-2431.
4. Gazder AA, Al-Harbi F, Spanke YT, Mitchel DRG, Pereloma EV. A correlative approach to segmenting phases and ferrite morphologies in transformation-induced plasticity steel using electron back-scattering diffraction and energy dispersive X-ray spectroscopy. *Ultramicroscopy*. 2014:147: 114-132.
5. Wright S, Nowell M, Field D. A Review of Strain Analysis Using Electron Backscatter Diffraction. *Microscopy and Microanalysis.* 2011;17(3): 316-329.
6. Zisman AA, Zolotorevsky NY, Petrov SN, Khlusova EI, Yashina EA. Panoramic crystallographic analysis of structure evolution in low-carbon martensitic steel under tempering. *Metal Science and Heat Treatment.* 2018;60: 142–149.
7. Lambert-Perlade A, Gourgues AF, Pineau A. Austenite to bainite phase transformation in the heat-affected zone of a high strength low alloy steel. *Acta Materialia*. 2004;52(8): 2337-2348.
8. Takayama N. Miyamoto G, Furuhara T. Effects of transformation temperature on variant pairing of bainitic ferrite in low carbon steel. *Acta Materialia*. 2012;60(5): 2387-2396.

9. Zolotorevskii NY, Zisman A, Panpurin S, Titovets YF, Golosienko S, Khlusova E. Effect of the grain size and deformation substructure of austenite on the crystal geometry of bainite and martensite in low-carbon steels. *Metal Science and Heat Treatment*. 2014;55: 550-558.
10. Zolotorevsky NY, Panpurin SN, Zisman AA, Petrov SN. Effect of ausforming and cooling condition on the orientation relationship in martensite and bainite of low carbon steels. *Materials Characterization*. 2015;107: 278-282.
11. Choi S. Model for estimation of transformation kinetics from the dilatation data during a cooling of hypoeutectoid steels. *Materials Science and Engineering*. 2003;A363: 72–80.
12. Van Bohemen SMC. Bainite and martensite start temperature calculated with exponential carbon dependence. *Materials Science and Technology*. 2012;28(4): 487-495.
13. Yakubtsov IA, Poruks P, Boyd JD. Microstructure and mechanical properties of bainitic low carbon high strength plate steels. *Materials Science and Engineering A.* 2008;480(1-2): 109–116.
14. Li Y, Chen S, Wang C, San Martín D, Xu W. Modeling retained austenite in Q&P steels accounting for the bainitic transformation and correction of its mismatch on optimal conditions. *Acta Materialia*. 2020;188: 528-538.
15. Liu M, Hu H, Kern M, Lederhaas B, Xu G, Bernhard C. Effect of integrated austempering and Q&P treatment on the transformation kinetics, microstructure and mechanical properties of a medium-carbon steel. *Materials Science and Engineering A*. 2023;869: 144780.
16. Yu H, Yu Y, Wang Z, Li F, Hu B, Liu S. On the variant pairing in transformation product of high strength low alloy steel depending on cooling rate. *Materials Letters.* 2022;326: 132953.

THE AUTHORS

Zisman A.A.
e-mail: crism_ru@yahoo.co.uk

Zolotorevsky N.Yu.
e-mail: zolotorevsky@phmf.spbstu.ru

Petrov S.N.
e-mail: epma@mail.ru

Ermakova N.Yu.
e-mail: ermakova@phmf.spbstu.ru